Ignition delay time measurements of methane and methane/ethane/propane mixtures with addition of ozone

Simon Drost, Robert Schießl, Ulrich Maas
Institute of Technical Thermodynamics, Karlsruhe Institute of Technology, KIT
76131 Karlsruhe, Germany

1   Introduction

Natural gas, with its high content of methane (CH_4), is the fossil fuel with the smallest carbon dioxide (CO_2) emission per energy of reaction ($\approx 0.055\,\mathrm{kg}$ CO_2 per $1\,\mathrm{MJ}$). Besides its availability from fossil sources, it can also be obtained from biomass or organic waste [1]. For this reason, natural gas and methane play important roles in terms of the change in the energy industry [2]. In current research, natural gas is investigated for various processes, such as: energy conversion processes [3, 4] or as a feedstock for the production of higher valued hydrocarbons [5].

Some of these processes operate under fuel-rich conditions [6, 7]. A homogeneous charge compression ignition (HCCI) engine can have advantages realizing these processes. However, natural gas is hard to ignite via compression, an ignition enhancer can be added, such as DME [8, 9], n-Heptane [9] or DEE [10]. Compared to natural gas, these substances have the disadvantage that they are expensive (more complex to produce and they have higher CO_2 emissions per unit of energy). A possible alternative accelerator is ozone (O_3), a highly reactive substance. It can be produced on site from atmospheric O_2 by plasma discharge (readily available in commercial ozone generators [11]).

Motivated by these advantages, in this study we investigate the auto-ignition of fuel-rich natural gas mixtures ($\phi = 2$), ignition accelerated by O_3 addition. The ignition delay times (IDT) are measured in a Rapid Compression Machine (RCM) at a compression pressure of $20\,\mathrm{bar}$, temperature range $T = 950$ to $1300\,\mathrm{K}$ and O_3 content of ≈ 310 to $910\,\mathrm{ppm}$.

2   Experimental setup

The experiments are performed in a Rapid Compression Machine (RCM), a piston-cylinder device for studying chemical reactions in compressed, hot gases under well-controlled conditions. An experiment is conducted according to the following procedure: First, the RCM combustion chamber is evacuated. and then filled with the gas to be investigated. This gas is then compressed by pushing the piston to top dead center. Because of its short compression time (approx. 20 - 40 ms), the compression is nearly adiabatic, and thus leads to high gas temperatures and pressures. The piston is mechanically locked when it reaches top dead center, such that isochoric conditions prevail afterwards. The compressed gas

can react and auto-ignition can occur. The strongly exothermal reactions after auto-ignition lead to a pronounced pressure rise when they occur under the isochoric conditions in the cylinder. By detecting the time-resolved in-cylinder pressure, the time between end of compression and the onset of the ignition-induced pressure rise can be determined experimentally (defined as ignition delay time, IDT). The experiment is described in more detail, including uncertainties and technical data in the following publications [10, 12, 13].

The investigated gas mixtures are created using the partial pressure method. The compositions are given in Table 1. When adding O_3, the amount of O_2 is reduced for a given equivalence ratio of 2. Since NG1 ignites faster than CH_4, less O_3 is added to the NG1 mixture.

Table 1: Experimental conditions investigated in this work.

No.	Fuel / mol-%			O_3 addition	Dilution D	Equivalence ratio ϕ
	CH_4	C_2H_6	C_3H_8			
1	100	-	-	-	90 mol-% Ar	2
2	90	9	1	-	90 mol-% Ar	2
3	100	-	-	$\approx 900\,\mathrm{ppm}$	90 mol-% Ar	2
4	90	9	1	$\approx 310\,\mathrm{ppm}$	90 mol-% Ar	2

The gas mixtures that are not very reactive (in this work pure CH_4 and natural gas surrogate (NG1: 90/9/1 CH_4/C_2H_6/C_3H_8, molar), each without O_3) are mixed in a vessel. In the case of O_3 addition, the reactivity is higher, and O_3 decomposes over several hours. For this reason, only fuel and argon are premixed in the mixing vessel for these measurements. O_2 and O_3 are filled in the combustion chamber first. Then, the fuel/Ar-mixture (about 95 mol-% of the total mixture) is added. The mixing time in the combustion chamber is about 1 min, however, a longer mixing time of 5 min did not affect the result. This indicates a homogeneous mixture.

O_3 is produced using an ozone generator (Ozone Solutions TG-40 [11]). The amount of O_3 is measured using the Flame UV-VIS Spectrometer from Ocean Insight, positioned directly in front of the combustion chamber. The initial temperatures were lower than 373 K. The amount of O_3 in the mixture was measured again after a longer waiting time (approx. 5 min.). Preoxidation or O_3 decay was not found here. A similar approach was found in the literature [14]. Simulations also show no decay of O_3 for these times and temperatures.

3 Simulations

The simulated IDTs are calculated with the in-house code HOMREA [15]. The reaction mechanism used to model the detailed chemistry consists of two mechanisms from the literature: UCB Chen reaction mechanism [12] for C1-C3 reactions (49 species and 332 reactions) and the Zhao O_3 sub-mechanism [16] for O_3 reactions (2 species and 11 reactions). The RCM with the heat losses is modeled based on calculated effective volume curves. To calculate the effective volume curves, non-reacting gas mixtures are compressed in the RCM and the pressure is measured. The effective volume is calculated via an isentropic relationship and the measured pressure [17]. Example pressure and volume-time curves can be seen in [18]. Simulation inputs are initial pressure and temperature, initial gas mixture, and the calculated effective volume curve.

4 Results

4.1 Validation of base case

Figure 1 (left) shows a comparison of pure CH_4 and a natural gas mixture (90/9/1 CH_4/C_2H_6/C_3H_8, molar), as described in Table 1 (No. 1 and 2). The ignition-accelerating effect of C_2H_6 and C_3H_8 is notable. The natural gas surrogate ignites at lower temperatures. Both mixtures show a linear behavior in the Arrhenius diagram, with a slightly steeper slope for pure CH_4. The UCB Chen reaction mechanism reproduces the IDTs of the mixtures diluted with $90\,\text{mol-}\%$ Ar; also the difference between CH_4 and NG (CH_4/C_2H_6/C_3H_8) is reproduced well. The UCB-Chen reaction mechanism has been validated using experiments from the literature covering multiple natural gas surrogates in combination with a wide pressure, temperature and equivalence ratio range [12].
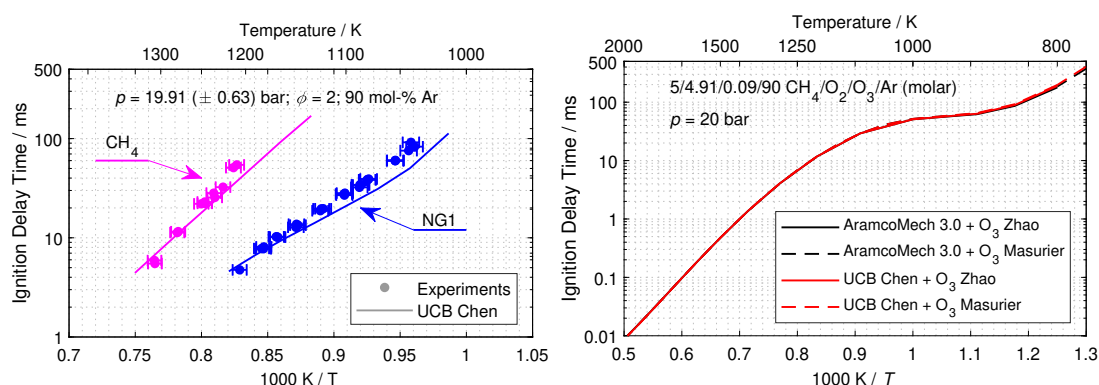
Figure 1: Left: IDTs of fuel-rich ($\phi = 2$) mixtures. Comparison between CH_4 and natural gas (NG1: 90/9/1 CH_4/C_2H_6/C_3H_8, molar) at a compression pressure of $p_c = 20\,\text{bar}$. Right: Comparison of IDTs, predicted by the reaction mechanisms AramcoMech 3.0 [19] + Zhao O_3 vs. UCB Chen + Zhao O_3.

Figure 1 (right) shows the comparison of IDTs calculated with the AramcoMech 3.0 in cobmination with the Zhao O_3 sub-mechanism as well as the reduced mechanism UCB Chen and the Zhao O_3 sub-mechanism. The UCB Chen reaction mechanism was developed based on the AramcoMech 3.0, with the target of reproducing the IDTs of natural gas mixtures. Both reaction mechanisms predict the same IDTs for the mentioned CH_4/O_2/O_3/Ar mixture. For this reason, only the results of the UCB Chen reaction mechanism are shown below.

4.2 Ignition delay times with ozone addition

Figure 2 compares IDTs of pure CH_4 and of CH_4 with O_3, as well as of a natural gas surrogate (NG1) and of NG1 with O_3. 910 (± 80) ppm O_3 was added to the CH_4 mixture, and 315 (± 32) ppm ppm to NG1. The addition of O_3 reduces the IDT in both cases. The experiments for CH_4 and CH_4 with O_3 were carried out under the same initial conditions (compression ratio and starting pressure). By adding O_3, an increased compression pressure was noticed. This indicates a reaction of O_3 during the compression phase. The RCM experiments can be compared via a constant compression pressure and variation of the compression temperatures [17]. In order to counteract the increased compression pressure caused by the addition of O_3, the initial pressure was reduced. We can rule out that O_3 reacts before compression starts (limited initial temperature, literature values, O_3 measurements, see section "Experimental setup"), but O_3 reacts during compression and thus leads to a higher compression pressure. The same behavior (no reaction of O_3 before compression, but increased compression pressure) was found for the NG1 mixture. The simulations with the corresponding volume curves derived from non-reacting mixtures showed no
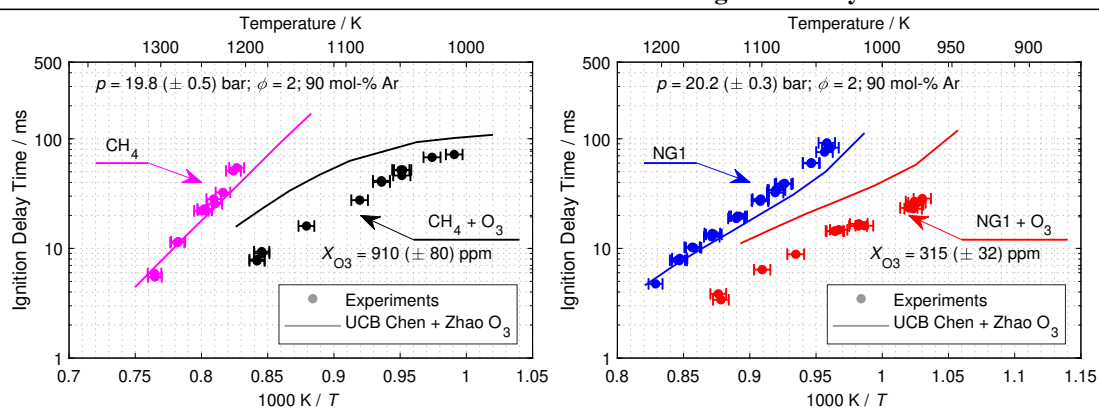
Figure 2: Left: Ignition delay times of CH_4 and O_3 addition. Right: Ignition delay times for natural gas surrogate (NG1: 90/9/1 CH_4/C_2H_6/C_3H_8, molar) and O_3 addition.

increase in the compression pressure. This suggests that the O_3 chemistry has a little influence on the compression pressure in the simulations and indicates that the reactivity of O_3 has too little influence in the simulations. This was confirmed with the IDTs that were predicted too long. Several considerations were followed in investigating this discrepancy: (a) Incorrectly determined temperature at the end of the compression in the experiments (validity of the adiabatic core and isentropic assumption and the reaction of O_3) (b) Incorrectly determined amount of O_3 before the experiment (c) Too low reactivity of O_3 in the reaction mechanism. The following chapter examines these three points in detail.

4.3   Discrepancy: experiments and simulations

The compression temperature in the experiments is calculated from the pressure in the experiments. Since the pressure is influenced by the chemical reaction of O_3, the calculated compression temperature can deviate from the actual real value. Under certain conditions (for example constant compression ratio), the experiments can also be compared via the initial temperatures. In this comparison, for example, the isentropic compression assumption is omitted. However, the comparison using the initial temperature instead the compression temperature did not show a better agreement between the experiments and simulations. For this reason, this result is not shown here. It can be concluded from this, that the temperature at top dead center may be influenced by the O_3 reaction during compression, but not so much that it can explain the deviation.

Figure 3 (left) shows IDTs that contain the uncertainty of the actual amount of O_3. The uncertainty of the initial amount of O_3 concentration is approx. $\pm$ 10 %. In Figure 3 (left) this is depicted by the black area, the upper limit with longer IDTs corresponds to the lower O_3 concentration, the lower boundary of the IDTs corresponds to the higher O_3 concentration in the initial mixture. Despite this uncertainty, the IDTs predicted by the simulation still do not match the IDTs of the experiments. An improved result would only be achieved when the amount of O_3 is doubled (dashed line).

The amount of O_3 over time shows an almost instantaneous O_3 consumption in the compression phase (concentration-time plot is not shown). A sensitivity analysis is performed for the time shortly before this sharp O_3 concentration decrease. It was found, that the reaction $O_3(+ M) \rightleftharpoons O_2 + O(+ M)$ is the most sensitive for the whole temperature range. The activation energy E_A, temperature exponent b and the pre-exponential factor A were varied for this reaction. A reduced activation energy leads to thermal decomposition of O_3 at lower temperatures, and this leads to slightly longer IDTs. For example, it turns out that if the temperature exponent b is reduced, the IDTs of the simulations and experiments agree better, especially at low temperatures. Figure 3 (right) shows the IDTs with the adjusted temperature
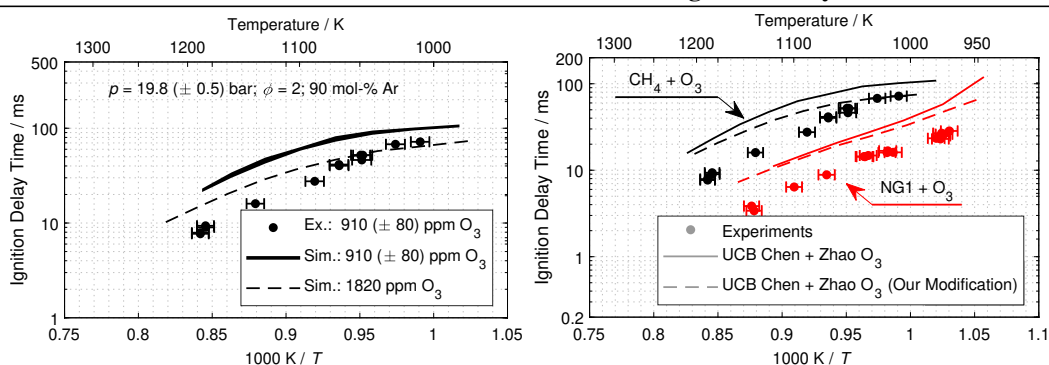
Figure 3: Left: Ignition delay times of CH_4 and $\approx 910\,\mathrm{ppm}$ O_3. Simulation data account for the uncertainty of O_3 (full line). Dashed line shows results obtained by the O_3 concentration doubled. Right: Ignition delay times of CH_4 + $\approx 910\,\mathrm{ppm}$ O_3 and natural gas surrogate (NG1: 90/9/1 $CH_4/C_2H_6/C_3H_8$, molar) + $\approx 315\,\mathrm{ppm}$ O_3. Dashed line shows simulation results with modified reaction $O_3(\,+\,M) \rightleftharpoons O_2 + O(\,+\,M)$. The temperature exponent is reduced to $b^* = -4.37$ from $b = -0.67$.

exponent (dotted lines) for CH_4 and NG1, each with O_3. However, this has a minor effect at the higher temperatures investigated. Furthermore, this reaction is already well investigated in literature [16] and an adaption simply to match the results is not recommended. Investigating the deviation between experiment and simulation, the influence of the compression temperature, the influence of the uncertainty of the ozone concentration, and the influence of the reaction of the thermal decomposition of O_3 were studied, whereby none of the three properties could explain the deviation at this point.

4   Conclusions

In this work, the ignition acceleration of O_3 on CH_4 and natural gas under fuel-rich conditions was investigated. The reaction mechanisms reflect the experimental observation of an accelerating effect of O_3 addition, but the reaction mechanism is unable to predict the exact IDTs; the reasons for this discrepancies are investigated. The reaction $O_3 + M$ to O_2 and O is the most important reaction for the O_3 decomposition. It has been found, that O_3 is consumed in a very short time in relation to the total IDT. Under the investigated conditions, the O_3 consumption takes place in the compression phase. The simulations show that the point in time of O_3 consumption during the compression phase and the speed of consumption have a major influence on the IDT. When adjusting the temperature exponent b in the Arrhenius equation of the mentioned reaction, it was found that the IDTs in particular are reproduced better at low temperatures, but because the rate coefficients of this reaction are quite well known, an adaptation beyond the experimental limits of uncertainties are not recommended. Most likely the discrepancies are due to the deficiencies in the model assumptions, in particular for the compression phase.

References

[1] A. Molino, F. Nanna, Y. Ding, B. Bikson, G. Braccio (2013). Biomethane production by anaerobic digestion of organic waste. Fuel, 103, pp. 1003 – 1009.

[2] M.A. MacKinnon, J. Brouwer, S. Samuelsen (2018). The role of natural gas and its infrastructure in mitigating greenhouse gas emissions, improving regional air quality, and renewable resource integration. Prog. Energy Combust. Sci., 64, pp. 62 – 92.W

[3] F. Crespi, G. Gavagnin, D. Sánchez, G. S. Martínez (2017). Supercritical carbon dioxide cycles for power generation: a review. Appl. Energy. 195, pp. 152 – 183.

[4] M. Sierra Aznar, F. Chorou , J. Y. Chen, A. Dreizler, R. W. Dibble (2019). Experimental and numerical investigation of the argon power cycle. Proc. ASME 2018 Intern. Combust. 1–10.

[5] S. Wiemann, R. Hegner, B. Atakan, C. Schulz, S. A. Kaiser (2018). Combined production of power and syngas in an internal combustion engine: experiments and simulations in SI and HCCI mode. Fuel, 215, pp. 40 – 45.

[6] A. Ashok, M. A. Katebah, P. Linke, D. Kumar, D. Arora, K. Fischer, T. Jacobs, M. Al-Rawashdeh (2021). Review of piston reactors for the production of chemicals. Rev. Chem. Eng.

[7] B. Atakan, S. A. Kaiser, J. Herzler, S. Porras, K. Banke, O. Deutschmann, T. Kasper, M. Fikri, R. Schießl, D. Schröder, C. Rudolph, D. Kaczmarek, H. Gossler, S. Drost, V. Bykov, U. Maas, C. Schulz (2021). Flexible energy conversion and storage via high-temperature gas-phase reactions: The piston engine as a polygeneration reactor. Renew. Sustain. Energy Rev. 133, 110264

[8] R. Hegner, M. Werler, R. Schießl, U. Maas, B. Atakan (2017). Fuel-Rich HCCI Engines as Chemical Reactors for Polygeneration: A Modeling and Experimental Study on Product Species and Thermodynamics. Energy Fuels, 31(12), pp. 14079 – 14088.

[9] J. Herzler, Y. Sakai, M. Fikri, C. Schulz (2019). Shock-tube study of the ignition and product formation of fuel-rich CH4/air and CH4/additive/air mixtures at high pressure. Proc. Combust. Inst., 37(4), pp. 5705 – 5713.

[10] S. Drost, M. Werler, R. Schießl, U. Maas (2021). Ignition delay times of methane/diethyl ether (DEE) blends measured in a rapid compression machine (RCM). J. Loss Prev. Process Ind. Vol. 71, No. 104430.

[11] Ozone Solutions (2019). TG Series - Air cooled ozone generator, Model: TG-10, 20, 40, Installation & operations manual. URL: https://ozonesolutions.com/content/TG-10-20-40_rev2a.pdf (Access: 20. Sept. 2021).

[12] S. Drost, M. Sierra Aznar, R. Schießl, M. Ebert, J. Y. Chen, U. Maas (2021). Reduced reaction mechanism for natural gas combustion in novel power cycles. Combust. Flame, 223, pp. 486 – 494.

[13] M. Werler, L. R. Cancino, R. Schiessl, U. Maas, and C. Schulz (2015). Ignition delay times of diethyl ether measured in a high-pressure shock tube and a rapid compression machine. Proc. Combust. Inst. Vol. 35, No. 1, pp. 259 - 266

[14] Y. Song, F. Foucher (2020). The impact of EGR components on ozone decomposition under engine relevant conditions in a rapid compression machine. Fuel, 276, 118009

[15] U. Maas, J. Warnatz (1988). Ignition processes in hydrogen-oxygen mixtures. Combust. Flame, 74(1), pp. 53 – 69.

[16] H. Zhao, X. Yang, Y. Ju (2016). Kinetic studies of ozone assisted low temperature oxidation of dimethyl ether in a flow reactor using molecular-beam mass spectrometry. Combust. Flame., 173, pp. 187-194

[17] S. S. Goldsborough, S. Hochgreb, G. Vanhove, M. S. Wooldridge, H. J. Curran, C. J. Sung (2017). Advances in rapid compression machine studies of low- and intermediate-temperature autoignition phenomena. Prog. Energy Combust. Sci. Vol. 63, pp. 1 - 78

[18] S. Drost, R. Schießl, M. Werler, J. Sommerer, U. Maas (2019). Ignition delay times of polyoxymethylene dimethyl ether fuels (OME2 and OME3) and air: Measurements in a rapid compression machine. Fuel, 258, 116070

[19] C. W. Zhou, Y. Li, U. Burke, C. Banyon, K. P. Somers, S. Ding, S. Khan, J. W. Hargis, T. Sikes, O. Mathieu, E. L. Petersen, M. AlAbbad, A. Farooq, Y. Pan, Y. Zhang, Z. Huang, J. Lopez, Z. Loparo, S. S. Vasu, H. J. Curran (2018). An experimental and chemical kinetic modeling study of 1,3-butadiene combustion: Ignition delay time and laminar flame speed measurements. Combust. Flame., 197, pp. 423 - 438.